ORIGINAL PAPER

Decolorization of reactive dyes by the white rot fungus *Phanerochaete velutina* in presence of Zn and ZnO nanoparticles

C. Zafiu[1] · S. Küpcü[2] · M. A. Kähkönen[3]

Abstract

Reactive organic dyes are hazardous pollutants that should be removed from wastewater from the textile industry. A remediation of dye polluted wastewater can be achieved by using the oxidative properties of nanomaterials, such as ZnO nanoparticles, or by microorganisms and their dye degrading enzymes. Promising approaches are expected from hybrid strategies, which use more than one approach. However, ZnO nanoparticles are also reported to be an antimicrobial and antifungal agent, which may undermine the decolorization ability of potent organisms, such as white rot fungi. Therefore, in this study we investigated the effects of soluble Zn and ZnO nanoparticles on the decolorization behaviour of the white rot fungus *Phanerochaete velutina* on commonly used reactive dyes, Reactive Orange 16 and Reactive Green 19. Zn ions led to a low decolorized rate of both dyes at low concentrations and restored the rate at higher Zn concentrations. However, ZnO nanoparticles showed highest decolorization rates, but only in a narrow concentration range. Overall, no toxic or inhibitory effects for decolorization of the dyes were found at the applied concentration of up to 20 mg Zn l^{-1} indicating that tolerant *P. velutina* will be suitable for remediation of dyes in multi polluted waste waters.

Keywords Zinc oxide · Nanoparticle · Pollution · White rot fungus · Decolorization · Reactive dyes

Introduction

Zinc oxide nanoparticles (ZnO-NP) are among the most frequently produced metal oxide nanoparticles with an annual production volume of 10^4–10^5 t in 2015 (Janković and Plata 2019). The materials are used mainly for cosmetic appliances, followed by coatings (Janković and Plata 2019). An important application is also food packaging, as ZnO-NP exhibit antimicrobial properties (Sirelkhatim et al. 2015).

These properties are associated to different mechanisms, such as the dissolution to Zn^{2+} ions and the catalytic production of reactive oxygen species (ROS) (Ann et al. 2014). However, these mechanisms are also potentially hazardous to algae, plants, invertebrates, vertebrates, and microorganisms (Ge et al. 2011; Hou et al. 2018; Shah et al. 2022). The antifungal properties of ZnO-NP were shown against ascomycetous *Sclerotinia homoeocarpa* (Li et al. 2017), *Aspergillus flavus*, and *Aspergillus niger* (Al-Dhabi and Valan Arasu 2018). These properties enable the ZnO-NP for the application as protective layers or for impregnating products made from wood (Bi et al. 2021; Clausen et al. 2009; Papadopoulos and Taghiyari 2019). Akhtari et al. (2013) showed that ZnO-NP inhibited the white rot fungus *Trametes versicolor* on wood from *Paulownia fortune*. ZnO-NP treated *Pinus sylvestris L.* was also protected against the ascomycetous fungi *Aspergillus niger*, *Trichoderma harzianum*, and *Penicillium pinophilum* (Terzi et al. 2016). In addition, ZnO-NP showed to have the most favorable properties compared to other wood protective nanoparticles (Kartal et al. 2009). Therefore, ZnO-NP, along with copper and silver-based nanoparticles, are currently strongly investigated as wood protection agents (Kora 2022; Reinprecht et al. 2022).

✉ C. Zafiu
christian.zafiu@boku.ac.at

1   Department of Water-Atmosphere-Environment (WAU), Institute of Waste Management and Circularity, University of Natural Resources and Life Sciences, Vienna, Muthgasse 107/3, 1190 Vienna, Austria

2   Department of Bionanosciences, Institute for Synthetic Bioarchitectures, University of Natural Resources and Life Sciences, Vienna, Muthgasse 11, 1190 Vienna, Austria

3   Department of Microbiology (Biocenter 1, Viikinkaari 9), Faculty of Agriculture and Forestry, University of Helsinki, Helsinki, Finland

🖄 Springer

From the studies on wood, it can be expected, that a toxic or inhibitory effect would also be found in aqueous media, which was not shown so far. Such data are interesting, as white rot fungi and their enzymes are researched for the depollution of wastewater, in particular such from the textile industry, due to their ability to degrade aromatic structures that can be persistent and toxic, like reactive textile dyes (Singh and Dwivedi 2020; Zafiu et al. 2021, 2022). In addition, ZnO-NP are investigated for their decolorization of effluent wastewater, and represent a promising approach (Danwittayakul et al. 2015; Dhatshanamurthi et al. 2017). Also, other physical, chemical, and biological approaches were investigated in the past and it was stated that one single technology won't be sufficient to effectively depollute industrial wastewater from reactive textile dyes (Hassan and Carr 2018). Therefore, a combined treatment by white rot fungi or their enzymes and ZnO-NP for reactive dye polluted wastewater could represent a novel solution. Due to the low rates, with half lives of days (Zafiu et al. 2021, 2022), to depollute wastewater by bioremediation, catalysis would be necessary for a practical application. However, it was also found that metals can cause an inhibition on fungi and their enzymes and lower the decolorization efficiency (Murugesan et al. 2007, 2009; Zafiu et al. 2021). This suggests that ZnO-NP could have either a synergistic catalytic or inhibitory impact on the decolorization ability of white rot fungi.

Therefore, this work aimed on assessing the inhibitory effects of ZnO-NP compared to soluble Zn on the decolorization of two commonly used reactive dyes, namely Reactive Orange 16 (RO-16) and Reactive Green 19 (RG-19) by the white rot fungus *Phanerochaete velutina*. This work was conducted at the Department of Microbiology (Biocenter 1, Viikinkaari 9), Faculty of Agriculture and Forestry, University of Helsinki (Finland) in 2022.

Materials and methods

Assay preparation

Zinc oxide nanoparticles (ZnO-NP) were purchased as a dispersion (50 wt% in H_2O, CAS 1314-13-2) and had a diameter of < 100 nm, with an average particle size of < 35 nm, which was measured by dynamic light scattering according to the manufacturer (Sigma-Aldrich: LOT MKBQ0692V). $ZnCl_2$ (Riedel de Haen, CAS 7646-85-7) was added in two different stock solutions in sterile low nitrogen asparagine-succinate (LN-AS) -solution with 0.5% (vol/ vol) glucose as carbon source. The LN-AS medium is referred to as the growth medium and had a pH of 4.5. The investigated white rot basidiomycetous fungus, *Phanerochaete velutina* (FBCC 941, old number 244i), was obtained from the Fungal Biotechnology Culture Collection (FBCC 941, old number 244i) at the Department of Microbiology of the University of Helsinki in Finland. *P. velutina* was pre-grown on malt extract agar plates for seven days at 28 °C. Five plugs (4 mm diameter) of pre-grown fungus on malt agar plates were added to two flasks (each 250 ml). These flasks contained 75 ml of sterilised growth medium. Both flasks were incubated and shaken at 28 °C for seven days (referred to pre-grown *P. velutina*).

The decolorization experiments were carried out in 24-microtiter plates. The stock solution of ZnO-NP and $ZnCl_2$ (150 mg Zn l^{-1}) were added in volumes to obtain final concentrations of 0, 100, 1000, 2500, 5000, 10,000 or 20,000 $\mu g\ l^{-1}$ referring to the Zn concentration of Zn-NP and $ZnCl_2$ in the growth medium. Growth medium was added to obtain a final volume of 460 µl in all wells. To these wells, 20 µl of sterile dye solution were added, which had a final concentrations of 100 mg l^{-1} in the wells. The investigated dyes were Reactive Orange 16 (RO-16; Sigma-Aldrich, Germany, CAS no. 12225-83-1) and Reactive Green 19 (RG-19; Sigma-Aldrich, Germany, CAS no. 12225-83-1). The experiment was started, when 20 µl of pre-grown *P. velutina* liquid culture was added aseptically to the wells. Control wells, without fungus or without the dyes, were filled with 20 µl sterile ultrapure water, instead of either the fungus or the dye, and had therefore a final volume of 500 µl. All experiments were prepared in triplicate and eight plates were prepared in total.

Absorbance measurements

The decolorization was measured after different times (0, 3, 7, 11, 14, and 20 days) as absorbance in a Tecan Infinite 200 plate reader (Tecan, Austria). The absorbance in experiments with RO-16 was measured at 504 nm, while experiments with RG-19 were measured at 630 nm. The plates were sealed and stored at 20 °C throughout the experiment.

Three different experimental setups were analysed by absorbance measurements in the plate readers. Control wells containing either $ZnCl_2$ or ZnO-NP at all investigated concentrations and without the dyes were prepared to investigate the background absorbance of either $ZnCl_2$ or ZnO-NP. The absorbance of the control was denominated as A_c. The second set of controls contained the fungus *P. velutina* and either $ZnCl_2$ or ZnO-NP at all investigated concentrations. This set was used to investigate the extent of the absorption increase, caused by the metabolic activity of the fungus (Zafiu et al. 2021, 2022). The absorbance contribution of the fungus was denominated as A_f. The third experimental set was the decolorization assay itself, that contained $ZnCl_2$ or ZnO-NP, the reactive dyes (either RO-16 or RG-19) and the *P. velutina*. The absorption obtained from this experiment (denominated A_{f+d}) is a superposition of both mechanisms, the absorption increase by the fungus metabolic activities

and the decolorization of the reactive dyes, as described in Zafiu et al. 2022. Therefore, the absorbance was calculated according to Eq. (1).

$$\Delta A = A_{f+d} - A_f \tag{1}$$

Kinetic calculations and statistical analysis

Zero (0), 1st, and 2nd order kinetic models were calculated for the decolorization reactions based on the initial absorbance A_0 (t = 0) and at the respective incubation time A_t with k as the rate constant using the linearized kinetic equations for 0 order (2), 1st order (3), and 2nd order (4) according to Ruscasso et al. (2021) and Sidney Santana et al. 2019. The best fit was assessed by comparing the linear regression coefficients (R^2) that were calculated in Excel 365 (Microsoft, USA). From all three fits the fit with an R^2 closest to 1 was considered as the best fit. For comparison the halve lives ($\tau_{1/2}$) were also calculated for 0 (5), 1st (6), and 2nd (7) order kinetic reactions.

$$A_0 - A_t = kt \tag{2}$$

$$-ln\frac{A_t}{A_0} = kt \tag{3}$$

$$\frac{1}{A_t} - \frac{1}{A_0} = kt \tag{4}$$

$$\frac{1}{2k}C_0 = \tau_{1/2} \tag{5}$$

$$\frac{\ln(2)}{k} = \tau_{1/2} \tag{6}$$

$$\frac{1}{C_0 k} = \tau_{1/2} \tag{7}$$

Statistical analysis for the determination of statistical significance of the data was performed in Sigma Plot 14.0.3 (Systat Software GmbH, Germany) using one- or two-way ANOVA with post-hoc Bonferroni test. Significance levels were defined as $p < 0.05$, $p < 0.01$, and $p < 0.001$, which were indicated in graphs by *, **, and ***, respectively.

Dose–response plots for the determination of inhibitory concentration IC_{50} values were fitted by Hill's type four parametric logistic curves (8), with absorption (A), minimum absorption (A_{min}), maximum absorption (A_{max}), the IC_{50} value (EC_{50}), the concentration of the metal salt (c), and the Hillslope (k_{Hill}). Dose-response caluculations were also made in Sigma Plot.

$$A = A_{min} + \frac{A_{max} - A_{min}}{1 + 10^{\log(EC_{50}-c)k_{Hill}}} \tag{8}$$

Optical microscopy

Samples were visualized in Nikon Eclipse Ts2R inverted fluorescence microscope (Nikon, Melville, NY). The images were taken with a 100 × oil immersion objective. For microscopy, a fraction of the samples was transferred on a glass slide and covered with a cover slip. No further staining was made. Fluorescence images were recorded by using a GFP-Fluorescence filter (Ex. 469 ± 35 nm; Em. 525 ± 39 nm).

Results and discussion

The absorbances obtained by the decolorization assay of the dye RO-16 with increasing amounts of $ZnCl_2$ and the respective controls are shown in Fig. 1. The control samples without *P. velutina* and without RO-16 exhibit an absorbance below 0.1 absorption units (a.u.), which was stable at all investigated concentrations of $ZnCl_2$ in the culture medium (A_c, Fig. 1a). Therefore, the interaction of Zn^{2+} with components of the culture medium did not cause an additional increase in the absorbance. When *P. velutina* was added to the growth medium without RO-16, an increasing absorbance was observed for all applied concentrations of $ZnCl_2$ and in the control (Fig. 1b). This observation was already described in an earlier study and was assigned to the metabolic or replicative processes of the fungus that indicates its vitality (A_f; Zafiu et al. 2022). The raw data from the decolorization assay in Fig. 1c shows decreasing absorbances at almost all concentrations of $ZnCl_2$, with exception of 100 and 5000 µg l^{-1}. However, the decreasing absorbances represent an overlay of the metabolic absorbance increase (A_{f+d} shown in Fig. 1b) by the fungus alone and the decolorization of the dye. Therefore, a subtraction of both signals was applied to obtain the pure decolorization data in Fig. 1d (Eq. (1)), as described in an earlier work (Zafiu et al. 2022). The subtracted absorbances (ΔA) featured decreasing trends, which became significant in the case of 10,000 µg l^{-1} of $ZnCl_2$ after 7 days and indicated that RO-16 was decolorized at all applied $ZnCl_2$ concentrations (detailed *p*-values are shown in Tables 1 and 2 in the supplementary information (SI)).

Figure 2 shows the absorbance data of experiments with *P. velutina* that was exposed to ZnO-NP. The control without ZnO-NP and the sample with a concentration of 2500 µg l^{-1} of ZnO-NP showed a constant background absorption < 0.1 a.u. (Fig. 2a), which was similar to the findings in the experiments with $ZnCl_2$ (comp. Fig. 1). At all other applied concentrations of ZnO-NP, an increasing absorption was
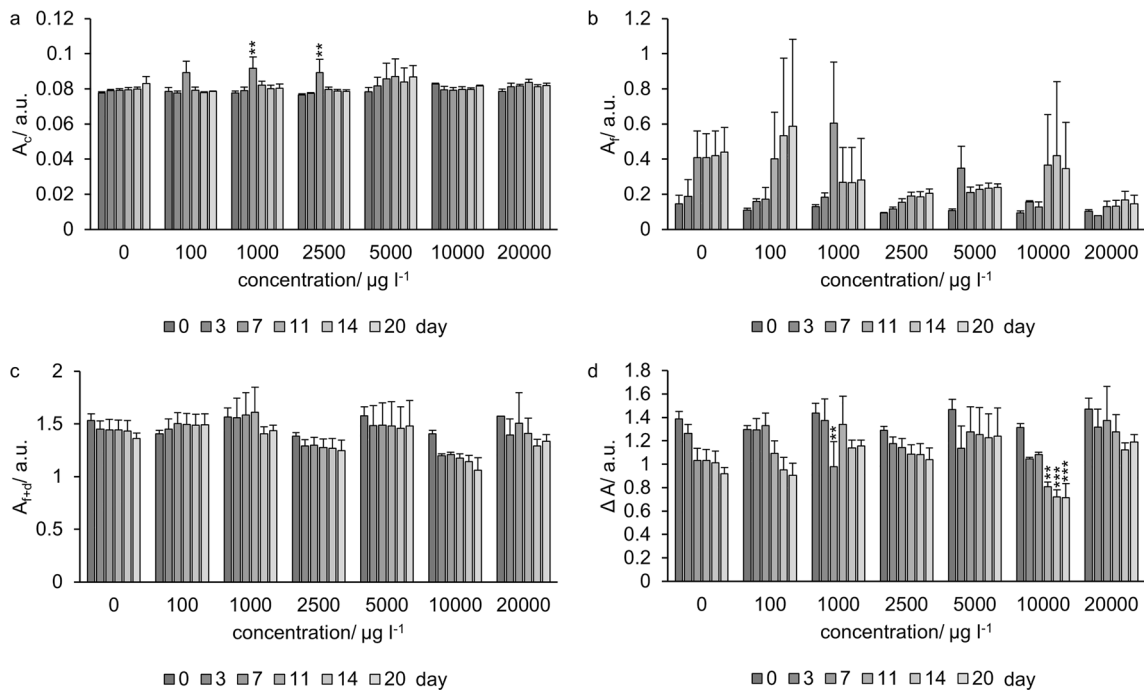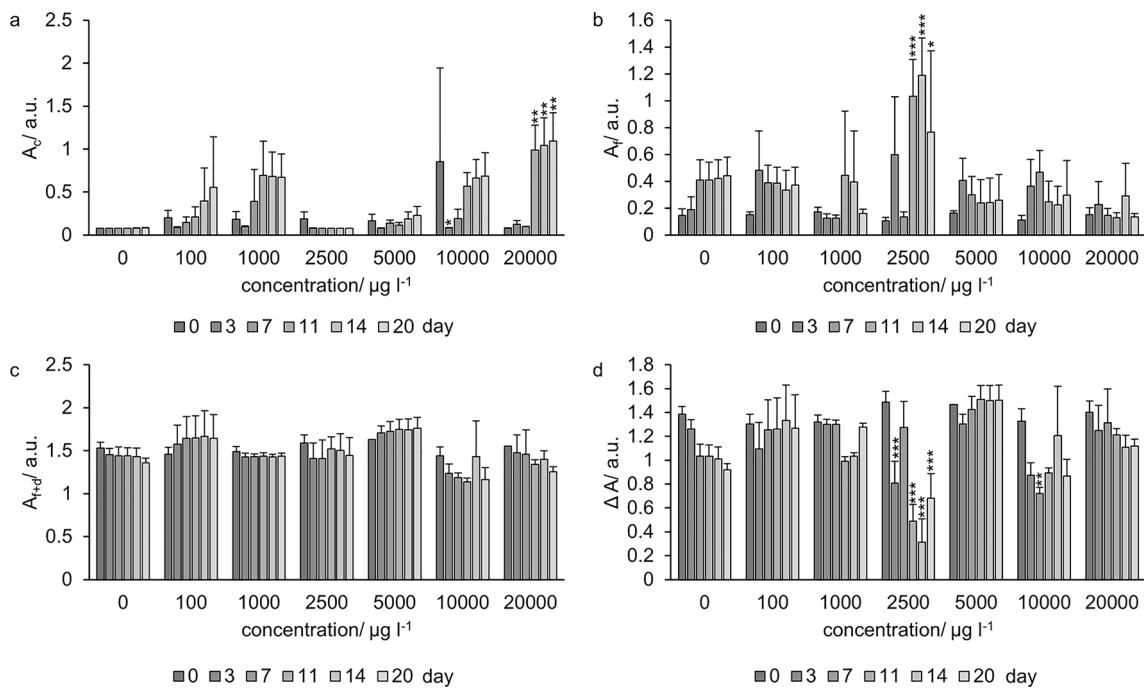
Fig. 1 Absorbance measurement at 504 nm after 0, 3, 7, 11, 14, and 20 days in experiments containing $ZnCl_2$. **a** Shows the control without the fungus and RO-16 (A_c), **b** shows only the fungus without RO-16 (A_f), **c** shows the decolorization experiments with the fungus and RO-16 (A_{f+d}), and d) shows the subtracted absorbance ΔA. Concentrations are given in µg Zn l^{-1}

Fig. 2 Absorbance measurement at 504 nm after 0, 3, 7, 11, 14, and 20 days in experiments containing ZnO-NP. **a** Shows the control without the fungus and RO-16 (A_c), **b** shows only the fungus without RO-16 (A_f), **c** shows the decolorization experiments with the fungus and RO-16 (A_{f+d}), and **d** shows the subtracted absorbance ΔA. Concentrations are given in µg Zn l^{-1}

found, which exceeded 1 a.u. in the case of the highest concentration (20,000 μg l^{-1}) after 11 days. This suggests that ZnO-NP was instable and its transformation, which was most likely by oxidation, in the culture medium led to the formation of compounds with a higher absorbance at 504 nm. When *P. velutina* was exposed to ZnO-NP (Fig. 2b) an absorption increase compared to day 0 could be observed at all applied concentrations with exception of the highest ZnO-NP concentration of 20,000 μg l^{-1}. The absorption increases indicate, that the fungus was vital at least when it was exposed to ZnO-NP concentration ≤ 10,000 μg l^{-1}. As already observed for ZnCl$_2$, a decolorization could only be observed in a few cases, such as at 20,000 μg l^{-1} (Fig. 2c). After the calculation of ΔA, the decolorization of RO-16 by *P. velutina* was shown for almost all concentrations of ZnO-NP (Fig. 2d).

The absorbance data of the pure decolorization (ΔA) of RO-16 were fitted by linearized zero, first and second order kinetic models to assess, which model fits best the observations by analyzing the regression coefficients and to obtain the rate constants from which, half lives were calculated for comparability (Table 3 in the SI; all results are shown in Tables 4 and 5 in the SI). However, the decolorization of RO-16 in the growth medium without any ZnCl$_2$ or ZnO-NP resulted in a rate constant of 0.02 d^{-1} (half-life $\tau_{1/2}$ of 35.4 d), which was lower than in earlier experiments with a rate constant of 0.05 d^{-1} and $\tau_{1/2}$ of 14.3 d for RO-16

(Zafiu et al. 2022). This finding indicates that the activity of the *P. velutina* was lower in the present experiments. For co-incubations with ZnCl$_2$ at most concentrations the decolorization followed first order kinetics, with two exceptions (1000 and 5000 μg l^{-1}). The half-lives of the control and the lowest concentration were almost the same at ca. 35 d. For higher concentrations they increased and dropped to a minimum of ca. 22 d for 10,000 μg l^{-1}, indicating the fastest degradation. Decolorization experiments with ZnO-NP co-incubation were mostly best described by zero order kinetic models. In case of 2500 μg l^{-1} the decolorization was best described by a first order model resulting in a higher decolorization rate than for ZnCl$_2$ with a half-life of ca. 13.5 d.

Similar investigations were made for the dye reactive green 19 (RG-19), which are shown in Fig. 3 for ZnCl$_2$, and Fig. 4 for ZnO-NP (detailed p values of all pair-wise comparisons are listed in Tables 6 and 7 in the SI). In these experiments, the calculations of absorbance increase and the decolorization were made in the same way as for RO-16. With respect to the kinetic parameters obtained from the absorbance data, a lower half life was found for RG-19, than for RO-16 in the control experiments without ZnCl$_2$ or ZnO-NP of ca. 25 d (Table 8 in the SI, detailed rate constants are shown in Tables 9 and 10 in the SI). In experiments where *P. velutina* was exposed to ZnCl$_2$ the halve lives were higher than the control, which indicates that ZnCl$_2$ was inhibiting the decolorization. The decolorization reaction was best
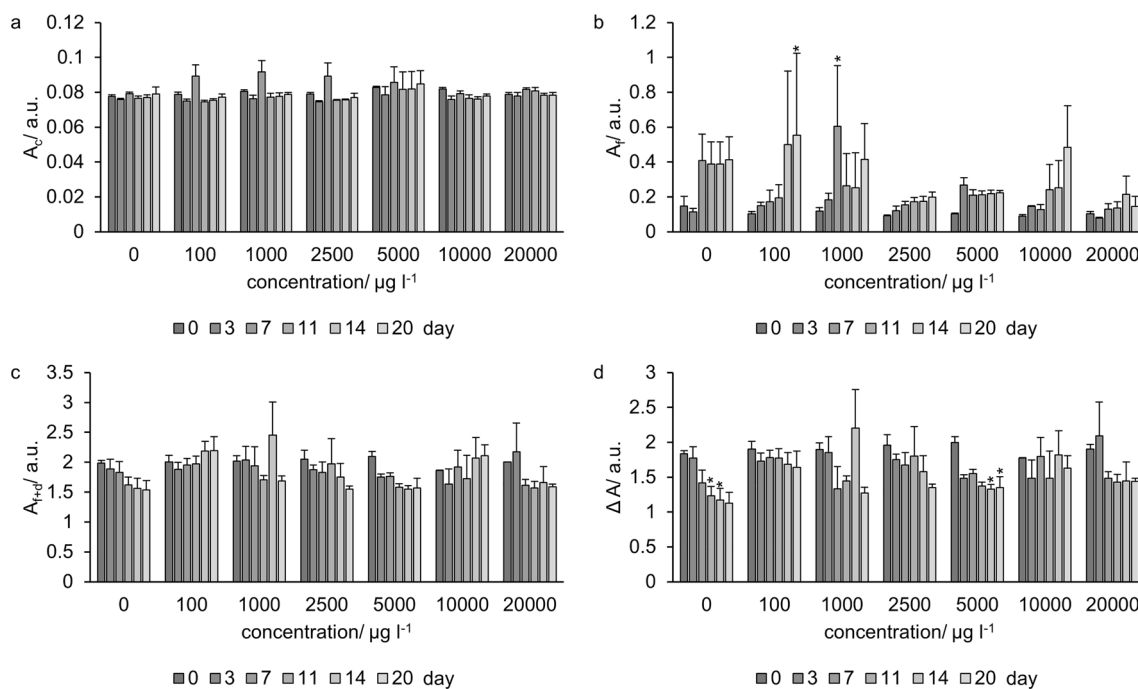

Fig. 3 Absorbance measurement at 630 nm after 0, 3, 7, 11, 14, and 20 days in experiments containing ZnCl$_2$. **a** Shows the control without the fungus and RG-19 (A$_c$), **b** shows only the fungus without RG-19 (A$_f$), **c** shows the decolorization experiments with the fungus and RG-19 (A$_{f+d}$), and **d** shows the subtracted absorbance ΔA. Concentrations are given in μg Zn l^{-1}
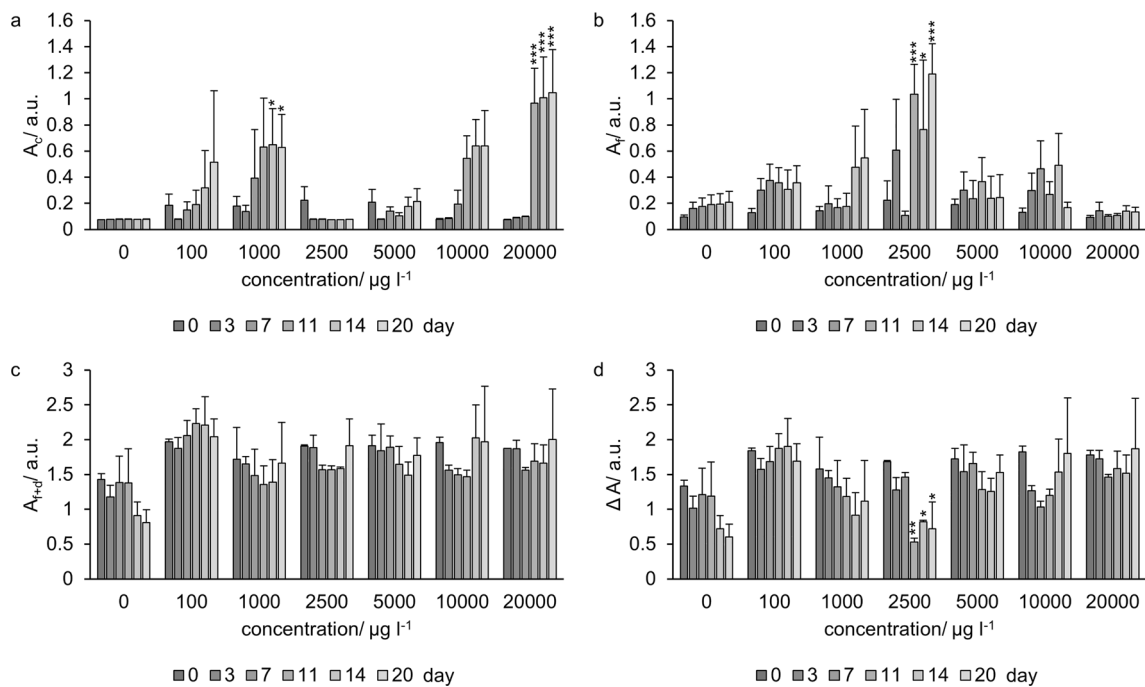
Fig. 4 Absorbance measurement at 630 nm after 0, 3, 7, 11, 14, and 20 days in experiments containing ZnO-NP. **a** Shows the control without the fungus and RG-19 (A_c), **b** shows only the fungus without RG-19 (A_f), **c** shows the decolorization experiments with the fungus and RG-19 (A_{f+d}), and **d** shows the subtracted absorbance ΔA. Concentrations are given in µg Zn l^{-1}

described by first order kinetic models for most exposure concentrations of $ZnCl_2$. However, the halve lives decreased towards higher concentrations, indicating that the inhibitory effect was found only for low concentrations (Table 6 in the SI). In the case of ZnO-NP, the decolorizations were best described by first order reactions for small concentrations of ZnO-NP. For concentrations ≥ 5000 µg l^{-1} the best fit was obtained by zero order models, which exhibited low R^2, indicating poor linearity that resulted in negative reaction constants. However, the poor linearity indicates that the decolorization process was inhibited in this concentration range. In contrast to ZnO-NP *P. velutina* exhibited the highest decolorization rate for RG-19 at 2500 µg l^{-1} with a half life of ca. 14.7 d. This half-life was lower than the control, which indicates that ZnO-NP at 2500 µg l^{-1} was accelerating the decolorization process.

Overall, the results show different inhibitory effects of $ZnCl_2$ or ZnO-NP on the decolorization of both dyes by *P. velutina*. For both dyes, low $ZnCl_2$ concentrations (< 2500 µg l^{-1}) inhibited the decolorization rate, which was restored at higher concentrations. In contrast, ZnO-NP increased the decolorization at a concentration of 2500 µg l^{-1} of both dyes. However, the decolorization rate was reduced at higher concentrations of ZnO-NP. This suggests that ZnO-NP acted synergistically on the decolorization of both dyes at 2500 µg l^{-1} and inhibited the decolorization at all other concentrations. For higher concentrations,

a strong toxic or inhibitory on *P. velutina* can be excluded, as calculation of dose response curves based on 4 parametric logistic curves (Hill equation) did not return significant results for both dyes for the absorbance increase data (Figs. 5, 6 and Tables 11, 12 in the SI) or the decolorization data (Figs. 7, 8 and Tables 13, 14 in the SI). Also, in case of $ZnCl_2$, no toxic or inhibitory effects could be found at any applied concentration according to the dose response curves. In an earlier study it was shown that Co and Ni co-pollutions inhibited the decolorization of RO-16 strongly (Zafiu et al. 2021), which couldn't be shown for Zn and ZnO-NP in case of RO-16 and RG-19 in this study.

The vitality of *P. velutina* after its exposure to $ZnCl_2$ and ZnO-NP was also investigated by fluorescence and bright field microscopy (Fig. 9 in the SI). Bright field images revealed the formation of mycelia and apparently intact cells in controls and after the exposure to 20,000 µg Zn l^{-1} $ZnCl_2$ or ZnO-NP. In fluorescence images, a strong autofluorescence could be observed in the control samples, which was not observed when *P. velutina* was exposed to $ZnCl_2$ or ZnO-NP. This finding indicates an influence of $ZnCl_2$ or ZnO-NP towards the ability of the fungus to form the (auto)fluorescent compounds, which could originate from cytochrome P450, such as reported by other authors (Da Coelho-Moreira et al. 2018; Ning et al. 2010; Wang et al. 2019). However, the ability to decolorize RO-16 and RG-19 was not altered by this interference, most probably

because extracellular enzymes were responsible for the decolorization.

Comparison with literature data

Literature data report that different bacteria and fungi species were shown to degrade textile dyes at a high efficiency, usually under optimized nutrition and temperature conditions. In particular, most of the studies were carried out in bioreactors and used stirring to distribute the cells and the dye well. For example, Fareed et al. shows that temperature can have a strong influence on the degradation efficiency of *Bacillus cereus* on reactive dyes (Fareed et al. 2022). They showed that the decolorization efficiency was at 100% at 37 °C compared to 40% at 30 °C for 100 mg l⁻¹ of RO-16. Ruscasso et al. reported a decolorization efficiency of ca. 94% at 20 °C after 48 h for 100 mg l⁻¹ of RO-16 by antarctic yeast in a pilot scale reactor under optimized conditions (Ruscasso et al. 2021). High decolorization rates were also found for yeast *Issatchenkia orientalis JKS6* which was able to decolorize 95–99% of RO-16 within 36 h by stirring at 32 °C (Jafari et al. 2014). These decolorization rates were higher than the ones obtained in this study, that were at highest at 34% for RO-16 and 55% for RG-19 after 20 days, which were obtained at a much lower temperature (20 °C), without stirring and in a non-optimized medium in relevant environmental conditions. However, the still promising results indicate that the *P. velutina* could have a higher potential for bioremediation, when the decolorization conditions are optimized, as was done by other authors. Moreover, ZnO-NP had, particularly at a concentration of 2500 μg l⁻¹, a positive effect on decolorization and improved the decolorization of RG-19 after 11 days from 11% without ZnO-NP to 69% with ZnO-NPs. For RO-16, the rate was even higher, with 79% (2500 μg l⁻¹ ZnO-NP), compared to 24% after 14 days. Under optimized temperature, stirring and nutrition conditions in a pilot scale bioreactor, the rate may be also improved to a few hours and bioremediation of wastewater made practical. However, the concentration of ZnO-NPs would have to be adjusted carefully, as the results show that the optimum is reached only in a very narrow concentration range. In addition, it is reported that the reactivity (e.g., adsorption properties) of ZnO-NP towards organic compounds (e.g., phenol) depend strongly on the type of their synthesis (see for review Dehmani et al. 2022). Since the synthesis was not disclosed by the manufacturer, it is unclear, if ZnO-NP from a different manufacturer may exhibit a higher synergistic effect on the decolorization, which could be only clarified by a systematic investigation of differently synthesized ZnO-NPs.

Conclusion

The present study shows that neither Zn, in its soluble form or dispersed as ZnO nanoparticles, strongly inhibits the decolorization of reactive dyes, RO-16 and RG-19. Thus, soluble Zn co-pollutions do not alter the decolorization of RO-16 and RG-19 performance of *P. velutina* for concentrations as high as 20,000 μg l⁻¹ (20 ppm). At ca. 2500 μg l⁻¹ ZnO-NP can increase the overall decolorization of both dyes by *P. velutina*. However, at lower or higher concentration of ZnO-NP the decolorization was lower than without Zn. Due to this limited concentration range of ZnO-NP a hybrid decolorization strategy for the depollution of dye contaminated wastewater by *P. velutina* and ZnO-NP can be achieved only by a precise control of the concentration of the nanoparticles. Such a concentration control would make the approach technically too complex, and most probably not economic with respect to other technologies, and would decolorize at best 50% of the dyes in approximately 13–15 d. In pilot scale reactors, that use agitation and optimized media in batch setups, the performance of the approached may be improved to a few hours and make the bioremediation of *P. velutina* in combination with ZnO-NP economically feasible.

Declarations

References

Akhtari M, Taghiyari HR, Kokandeh MG (2013) Effect of some metal nanoparticles on the spectroscopy analysis of Paulownia wood exposed to white-rot fungus. Eur J Wood Prod 71:283–285. https://doi.org/10.1007/s00107-013-0676-5

Al-Dhabi NA, Valan Arasu M (2018) Environmentally-friendly green approach for the production of zinc oxide nanoparticles and their anti-fungal, ovicidal, and larvicidal properties. Nanomaterials (Basel, Switzerland) 8. https://doi.org/10.3390/nano8070500

Ann LC, Mahmud S, Bakhori SKM, Sirelkhatim A, Mohamad D, Hasan H, Seeni A, Rahman RA (2014) Antibacterial responses of zinc oxide structures against *Staphylococcus aureus*, *Pseudomonas aeruginosa* and *Streptococcus pyogenes*. Ceram Int 40:2993–3001. https://doi.org/10.1016/j.ceramint.2013.10.008

Bi W, Li H, Hui D, Gaff M, Lorenzo R, Corbi I, Corbi O, Ashraf M (2021) Effects of chemical modification and nanotechnology on wood properties. Nanotechnol Rev 10:978–1008. https://doi.org/10.1515/ntrev-2021-0065

Clausen CA, Yang VW, Arango RA, Green F III (2009) Feasibility of nanozinc oxide as a wood preservative. In: Proceedings of the one hundred fifth annual Meeting of the American Wood Protection Association, pp 255–260

Da Coelho-Moreira JS, Brugnari T, Sá-Nakanishi AB, Castoldi R, de Souza CGM, Bracht A, Peralta RM (2018) Evaluation of diuron tolerance and biotransformation by the white-rot fungus *Ganoderma lucidum*. Fungal Biol 122:471–478. https://doi.org/10.1016/j.funbio.2017.10.008

Danwittayakul S, Jaisai M, Dutta J (2015) Efficient solar photocatalytic degradation of textile wastewater using ZnO/ZTO composites. Appl Catal B 163:1–8. https://doi.org/10.1016/j.apcatb.2014.07.042

Dehmani Y, Dridi D, Lamhasni T, Abouarnadasse S, Chtourou R, Lima EC (2022) Review of phenol adsorption on transition metal oxides and other adsorbents. J Water Process Eng 49:102965. https://doi.org/10.1016/j.jwpe.2022.102965

Dhatshanamurthi P, Shanthi M, Swaminathan M (2017) An efficient pilot scale solar treatment method for dye industry effluent using nano-ZnO. J Water Process Eng 16:28–34. https://doi.org/10.1016/j.jwpe.2016.12.002

Fareed A, Zaffar H, Bilal M, Hussain J, Jackson C, Naqvi TA (2022) Decolorization of azo dyes by a novel aerobic bacterial strain Bacillus cereus strain ROC. PLoS ONE 17:e0269559. https://doi.org/10.1371/journal.pone.0269559

Ge Y, Schimel JP, Holden PA (2011) Evidence for negative effects of TiO2 and ZnO nanoparticles on soil bacterial communities. Environ Sci Technol 45:1659–1664. https://doi.org/10.1021/es103040t

Hassan MM, Carr CM (2018) A critical review on recent advancements of the removal of reactive dyes from dyehouse effluent by ion-exchange adsorbents. Chemosphere 209:201–219. https://doi.org/10.1016/j.chemosphere.2018.06.043

Hou J, Wu Y, Li X, Wei B, Li S, Wang X (2018) Toxic effects of different types of zinc oxide nanoparticles on algae, plants, invertebrates, vertebrates and microorganisms. Chemosphere 193:852–860. https://doi.org/10.1016/j.chemosphere.2017.11.077

Jafari N, Soudi MR, Kasra-Kermanshahi R (2014) Biodecolorization of textile azo dyes by isolated yeast from activated sludge: Issatchenkia orientalis JKS6. Ann Microbiol 64:475–482. https://doi.org/10.1007/s13213-013-0677-y

Janković NZ, Plata DL (2019) Engineered nanomaterials in the context of global element cycles. Environ Sci Nano 6:2697–2711. https://doi.org/10.1039/C9EN00322C

Kartal SN, Green F, Clausen CA (2009) Do the unique properties of nanometals affect leachability or efficacy against fungi and termites? Int Biodeterior Biodegrad 63:490–495. https://doi.org/10.1016/j.ibiod.2009.01.007

Kora AJ (2022) Chapter 6—Copper-based nanopesticides. In: Abd-Elsalam KA (ed) Copper nanostructures. Elsevier, San Diego, pp 133–153

Li J, Sang H, Guo H, Popko JT, He L, White JC, Parkash Dhankher O, Jung G, Xing B (2017) Antifungal mechanisms of ZnO and Ag nanoparticles to *Sclerotinia homoeocarpa*. Nanotechnology 28:155101. https://doi.org/10.1088/1361-6528/aa61f3

Murugesan K, Nam I-H, Kim Y-M, Chang Y-S (2007) Decolorization of reactive dyes by a thermostable laccase produced by *Ganoderma lucidum* in solid state culture. Enzyme Microb Technol 40:1662–1672. https://doi.org/10.1016/j.enzmictec.2006.08.028

Murugesan K, Kim Y-M, Jeon J-R, Chang Y-S (2009) Effect of metal ions on reactive dye decolorization by laccase from *Ganoderma lucidum*. J Hazard Mater 168:523–529. https://doi.org/10.1016/j.jhazmat.2009.02.075

Ning D, Wang H, Zhuang Y (2010) Induction of functional cytochrome P450 and its involvement in degradation of benzoic acid by *Phanerochaete chrysosporium*. Biodegradation 21:297–308. https://doi.org/10.1007/s10532-009-9301-z

Papadopoulos AN, Taghiyari HR (2019) Innovative wood surface treatments based on nanotechnology. Coatings 9:866. https://doi.org/10.3390/coatings9120866

Reinprecht L, Repák M, Iždinský J, Vidholdová Z (2022) Decay resistance of nano-zinc oxide, and PEG 6000, and thermally modified wood. Forests 13:731. https://doi.org/10.3390/f13050731

Ruscasso F, Cavello I, Butler M, Loveira EL, Curutchet G, Cavalitto S (2021) Biodegradation and detoxification of reactive orange 16 by Candida sake 41E. Bioresource Technol Reports 15:100726. https://doi.org/10.1016/j.biteb.2021.100726

Shah GM, Ali H, Ahmad I, Kamran M, Hammad M, Shah GA, Bakhat HF, Waqar A, Guo J, Dong R, Rashid MI (2022) Nano agrochemical zinc oxide influences microbial activity, carbon, and nitrogen cycling of applied manures in the soil-plant system. Environ Pollut 293:118559. https://doi.org/10.1016/j.envpol.2021.118559

Singh G, Dwivedi SK (2020) Decolorization and degradation of Direct Blue-1 (Azo dye) by newly isolated fungus *Aspergillus terreus* GS28, from sludge of carpet industry. Environ Technol Innov 18:100751. https://doi.org/10.1016/j.eti.2020.100751

Sirelkhatim A, Mahmud S, Seeni A, Kaus NHM, Ann LC, Bakhori SKM, Hasan H, Mohamad D (2015) Review on zinc oxide nanoparticles: antibacterial activity and toxicity mechanism. Nano-Micro Lett 7:219–242. https://doi.org/10.1007/s40820-015-0040-x

Terzi E, Kartal SN, Yılgör N, Rautkari L, Yoshimura T (2016) Role of various nano-particles in prevention of fungal decay, mold growth and termite attack in wood, and their effect on weathering properties and water repellency. Int Biodeterior Biodegradation 107:77–87. https://doi.org/10.1016/j.ibiod.2015.11.010

Wang J, Ohno H, Ide Y, Ichinose H, Mori T, Kawagishi H, Hirai H (2019) Identification of the cytochrome P450 involved in the degradation of neonicotinoid insecticide acetamiprid in *Phanerochaete chrysosporium*. J Hazard Mater 371:494–498. https://doi.org/10.1016/j.jhazmat.2019.03.042

Zafiu C, Part F, Ehmoser E-K, Kähkönen MA (2021) Investigations on inhibitory effects of nickel and cobalt salts on the decolorization

of textile dyes by the white rot fungus *Phanerochaete velutina*. Ecotoxicol Environ Saf 215:112093. https://doi.org/10.1016/j.ecoenv.2021.112093

Zafiu C, Küpcü S, Kähkönen MA (2022) Method to determine the decolorization potential of persistent dyes by white rot fungi by colorimetric assays. Methods X 9:101885. https://doi.org/10.1016/j.mex.2022.101885